Talin-Null Cells of *Dictyostelium* Are Strongly Defective in Adhesion to Particle and Substrate Surfaces and Slightly Impaired in Cytokinesis

Jens Niewöhner, Igor Weber, Markus Maniak, Annette Müller-Taubenberger, and Günther Gerisch

Max-Planck-Institut für Biochemie, D-82152 Martinsried, Germany

Abstract. *Dictyostelium discoideum* contains a full-length homologue of talin, a protein implicated in linkage of the actin system to sites of cell-to-substrate adhesion in fibroblasts and neuronal growth cones. Gene replacement eliminated the talin homologue in *Dictyostelium* and led to defects in phagocytosis and cell-to-substrate interaction of moving cells, two processes dependent on a continuous cross talk between the cell surface and underlying cytoskeleton. The uptake rate of yeast particles was reduced, and only bacteria devoid of the carbohydrate moiety of cell surface lipopolysaccharides were adhesive enough to be recruited by talin-null cells in suspension and phagocytosed. Cell-to-cell adhesion of undeveloped cells was strongly impaired in the absence of talin, in contrast with the cohesion of aggregating cells mediated by the phospholipid-anchored contact site A glycoprotein, which proved to be less talin dependent. The mutant cells were still capable of moving and responding to a chemoattractant, although they attached only loosely to a substrate via small areas of their surface. With their high proportion of binucleated cells, the talin-null mutants revealed interactions of the mitotic apparatus with the cell cortex that were not obvious in mononucleated cells.

THE surface of a motile cell receives signals upon contact with another surface, and transmits these signals through the plasma membrane to accommodate activities of the underlying actin system. The array of actin filaments, which acts as a target, is furnished with myosin motors of various types, as well as with other proteins that regulate actin polymerization or the cross-linkage and connection of actin filaments with the plasma membrane. The actin system is not only a target of signals arising in the environment of a cell; it modulates in turn the interactions of a cell with an extracellular matrix or with another cell. One of the proteins that link the plasma membrane to the actin skeleton is talin (Burridge and Connell, 1983). In fibroblasts, talin acts in concert with other adhesion plaque proteins in anchoring stress fibers to integrin clusters in the plasma membrane (Horwitz et al., 1986; Lewis and Schwartz, 1995). On the outside, these clusters are connected to fibronectin or laminin, thus associating the cells with the extracellular matrix (for review see Geiger et al., 1995; Jockusch et al., 1995). In motile fibroblasts, talin accumulates also in membrane ruffles at the leading edge (Hock et al., 1989; DePasquale and Izzard, 1991).

Human platelet and chicken gizzard talins are considered to be antiparallel homodimers (Goldmann et al., 1994) or flexible monomers that partially associate into parallel dimers (Winkler et al., 1997). Talin binds directly to actin (Muguruma et al., 1990), vinculin (Burridge and Mangeat, 1984), and β integrins (Horwitz et al., 1986; Knezevic et al., 1996). In the subunits of chicken talin, three actin-binding sites linked to three vinculin-binding sites can be distinguished (Hemmings et al., 1996). Talin nucleates actin polymerization (Kaufmann et al., 1991; Isenberg et al., 1996), cross-links actin filaments (Zhang et al., 1996), and anchors these filaments at membranes (Kaufmann et al., 1992). The β integrin, but not vinculin, is essential for the assembly of talin at focal adhesions (Moulder et al., 1996). With its NH_2-terminal domain, comprising a region typical of ezrin-radixin-moesin family proteins (Takeuchi et al., 1994), talin can bind to membrane lipids (Niggli et al., 1994).

Evidence that talin plays a major role in the interplay between membrane proteins and the submembraneous cytoskeleton has been accumulated. Talin is enriched in phagocytic cups during F_C receptor–mediated particle uptake (Greenberg et al., 1990), and is also enriched in contact areas between T-helper and antigen-presenting cells (Kupfer et al., 1987). Downregulation of talin by antisense RNA reduces the speed of cell spreading, the size of focal contacts, and the formation of stress fibers (Albigès-Rizo et al., 1995). Similarly, microinjection of anti-talin antibodies inhibits the spreading of fibroblasts on a fibronectin substrate (Nuckolls et al., 1992). In neuronal growth

Please address all correspondence to Günther Gerisch, Max-Planck-Institut für Biochemie, Abteilung Zellbiologie, D-82152 Martinsried, Germany. Tel.: (49) 89-8578-2326. Fax: (49) 89-8578-3885. e-mail: gerisch@biochem.mpg.de

cones, chromophore-assisted laser inactivation of talin results in the cessation of both extension and retraction of filopods, suggesting that talin couples signals generated in substrate-attached filopods to actin-filament dynamics (Sydor et al., 1996).

Cells of *Dictyostelium discoideum* interact during their life cycle with three types of surfaces: with bacteria or other microorganisms that are phagocytosed as a food, with substrates on which the cells are ready to move, and with cells of the same species to build a multicellular organism by aggregation. The highly motile cells of this microorganism are distinguished from fibroblasts by the absence of stress fibers and adhesion plaques that would stabilize cell shape and substrate interaction. *D. discoideum* is the first nonmetazoan known to contain a full-length talin homologue. In undifferentiated cells, this 269-kD talin homologue is strongly accumulated at the tips of filopods, and in aggregating cells it accumulates at the leading edge in a chemoattractant-controlled manner (Kreitmeier et al., 1995).

With the possibility in mind that *Dictyostelium* cells make less specialized and less complicated adhesion complexes than fibroblasts, we have eliminated talin in *D. discoideum* by gene replacement. The talin-null cells moved with small patches of their surface loosely adhering to a substrate, indicating that cell motility is essentially independent in *Dictyostelium* of traction forces or of a gradient in substrate adhesiveness established between the front and tail of a cell. The absence of talin markedly affected the first steps of phagocytosis in cell suspensions where particle attachment to the cell surface was critical for uptake. A slight impairment of cytokinesis observed in talin-null cells indicated that talin assists in the changes of cell shape that lead to the separation of daughter cells.

Materials and Methods

Growth and Development of D. discoideum Cells

For axenic growth, *D. discoideum* wild-type strain AX2 and talin-null mutants were cultivated in shaken suspension at 150 rpm in liquid nutrient medium at 23°C as described by Claviez et al. (1982). For starvation, cells were washed twice in 17 mM K-Na phosphate buffer, pH 6.0 (non-nutrient buffer) and were shaken at a density of 10^7 cells per ml in the buffer. To achieve aggregation competence, AX2 cells were starved for 6 h, and talin-null cells were starved for 8 h.

For growth in bacterial suspensions, *Escherichia coli B/r* or *Salmonella minnesota R595* were cultivated overnight in standard I nutrient broth (Merck, Darmstadt, Germany), washed, and adjusted to a density corresponding to 10^{10} *E. coli B/r* cells per ml. The suspensions of washed bacteria were inoculated with 10^4–10^5 cells of *D. discoideum* per ml. For cultivation on agar surfaces, cells of *E. coli B/r* were spread on agar plates containing 0.1% peptone and 0.1% glucose in non-nutrient buffer. AX2 or talin-null cells were picked onto the surface for measuring radial growth.

Experiments shown in Fig. 3 were performed with the talin-null mutant strain HG1664 and repeated with HG1666. Experiments in Figs. 2, 4, 5, and 6 were performed with the talin-null strain HG1666 and repeated with HG1663 (see Fig. 2), HG1664 (see Fig. 4, *B/r* suspension), or HG1665 (see Figs. 5 and 6). The micrographs of cytokinesis and immunofluorescence images of Fig. 7 were obtained with mutant HG1665.

Gene Replacement in D. discoideum

The targeting vector was constructed by inserting the Bsr cassette from plasmid pBsr2 (Sutoh, 1993) into the single blunted PstI site of a genomic DNA fragment comprising base pairs 58–3,031 of the talin coding region. This fragment was obtained by PCR using primers 5′-GCGGATCCTTTGCACCAGATATGTGTATTC and 3′-CGGCAATTCAACTTAGC, and was cloned into pUC19. The construct was excised using BamHI and HindIII, and the linearized and dephosphorylated fragment was used to transfect AX2 wild-type cells of *D. discoideum* by electroporation. Talin-null mutants were selected with 7.5 μg/ml blasticidin S (ICN Biomedicals, Inc., Costa Mesa, CA) in nutrient medium.

For Southern blotting, genomic DNA was prepared according to Noegel et al. (1985). 15 μg of either AX2 or mutant DNA was run on 1% agarose gels and blotted onto Hybond N nylon membrane (Amersham Intl., Little Chalfont, UK). The blots were hybridized under high stringency for 15 h at 65°C in RapidHyb buffer (Amersham Intl.) with a PCR-generated probe comprising base pairs 3,086–3,442 of the talin coding region.

Monoclonal Antibodies

mAb 477 against *D. discoideum* talin was produced by Kreitmeier et al. (1995). The antibody recognized an epitope between amino acid residues 2,053 and 2,290, as deduced from bacterially expressed talin polypeptide fragments. mAb 227-341-4 (here designated as mAb 341) was obtained from a *Balb/c* mouse immunized with a His-tagged NH_2-terminal fragment comprising residues 20–124 of the talin sequence. For the production of this fragment, a genomic DNA fragment was generated by PCR and cloned into pQE30 (QIAGEN Inc., Chatsworth, CA). The sequence was verified and the fragment was expressed in *E. coli M15.* The protein was purified on a Ni^{2+}-agarose column under denaturing conditions using 6 M guanidinium chloride followed by 8 M urea. The fragment was injected together with Freund's adjuvant, and spleen cells were fused with $PAIB_3Ag81$ myeloma cells.

SDS-PAGE and immunoblotting with anti-talin antibodies was performed in 3–20% gradient polyacrylamide gels. mAb 477 was directly ^{125}I-labeled, and mAb 341 was detected with iodinated sheep anti–mouse IgG (Amersham Intl.). For detection of the csA glycoprotein on Western blots, mAb 294 was used (Bertholdt et al., 1985).

Reflection Interference Contrast Microscopy/Bright-Field Double-View Microscopy and Chemotactic Stimulation

Aggregation-competent *Dictyostelium* cells were monitored while migrating on the surface of a glass coverslip preincubated with 0.2% BSA solution (Serva, Heidelberg, Germany). The topography of the ventral cell surface, including cell-to-substratum contacts, was imaged by reflection interference contrast microscopy (RICM)[1] using a double-view microscope (Weber et al., 1995). The wavelength of the green light used for RICM was $\lambda = 546$ nm. Contours of two-dimensional projections of the cell body, as seen in bright-field images, were extracted by an image processing routine (Weber and Albrecht, 1997) and superimposed onto the RICM images. Chemotactic responses were recorded while the cells were stimulated from a micropipette filled with a solution of 10^{-4} M cAMP and placed with its orifice at a distance of 10–20 μm from the cell surface (Gerisch and Keller, 1981).

Cell Agglutination and Endocytosis Assays

Agglutination of wild-type and talin-null cells was assayed by measuring light scattering according to Beug and Gerisch (1972) in a microprocessor-controlled agglutinometer (Bozzaro et al., 1987). Phagocytosis assays using TRITC-labeled heat-killed yeast in shaken suspension were carried out essentially as described by Maniak et al. (1995), and quantitative and microscopic assays of fluid-phase uptake were performed using TRITC-labeled dextran according to Hacker et al. (1997). For the quantitative assays of Fig. 3, *A–C*, and Fig. 5, *A* and *C*, suspensions of wild-type and talin-null cells were adjusted to the same total cell volume by determining the volume of densely packed cells (Maniak et al., 1995). The volume of the mutant cells was, on the average, 1.5-fold the volume of wild-type cells.

Analysis of Cytokinesis

For synchronization, cells from suspension cultures were washed and shaken in non-nutrient buffer for 3 h, before they were allowed to adhere

1. *Abbreviations used in this paper*: DAPI, 4′,6-diamidino-2-phenylindole; RICM, reflection interference contrast microscopy.

for 30 min on glass coverslips. Subsequently, the buffer was replaced by nutrient medium and the culture continued for 4 h (Neujahr et al., 1997). Cytokinesis in the adherent cells was monitored by video recording. For fluorescence labeling, the cells were fixed for 15 min in a solution of 15% saturated picric acid, 2% paraformaldehyde, pH 6.0, postfixed with 70% ethanol, and processed according to Humbel and Biegelmann (1992). α-Tubulin was labeled with rat mAb YL 1/2 (Kilmartin et al., 1982) and TRITC-conjugated goat anti–rat antibodies (Jackson ImmunoResearch Laboratories, Inc., West Grove, PA). DNA was stained with 4′,6-diamidino-2-phenylindole (DAPI) (Sigma, Deisenhofen, Germany). Micrographs were taken with a Phaco ×100 oil Neofluar objective using a Zeiss Axiophot microscope (Oberkochen, Germany).

Results

Knockout of a Talin Homologue in Dictyostelium

To inactivate the gene that encodes the *Dictyostelium* talin previously described by Kreitmeier et al. (1995), cells of *D. discoideum* were transfected with a vector causing gene replacement by homologous recombination. The vector was designed to interrupt the gene by a blasticidin resistance (bsr) cassette at the codon for T516 of the talin sequence (Fig. 1 *A*). Probing 40 blasticidin-resistant clones by Southern blotting revealed eight independent transformants in which the gene was disrupted. These mutant lines were characterized by two phenotypic alterations: (*a*) weak adhesion to the polystyrene surfaces of petri dishes, and (*b*) the tendency to form larger cells in suspension. All transformants completed development on agar with the formation of normal fruiting bodies.

In all of the eight mutants obtained, the vector was selectively inserted into the talin gene; no second insertion into other regions of the genome had occurred. In Fig. 1, *B* and *C*, data for four of these mutants are shown. EcoRV and BclI cut the gene at both sides of the inserted bsr cassette. When genomic DNA of the mutants was digested with either one of these two enzymes and probed with a sequence stretch of the talin gene downstream of the vector sequence, single bands were labeled. These bands indicated an increase in size by 1.4 kb relative to the wild-type fragments, an upshift that corresponds to the size of the bsr cassette (Fig. 1 *B*, *upper panels*). Using as a probe the bsr coding region of the vector, the same single bands showed up in the mutants. As expected, no hybridization signal was seen with wild-type DNA (Fig. 1 *B*, *lower panels*).

Western blots of total cellular proteins separated by SDS-PAGE were probed with two antibodies, one binding COOH-terminally to the predicted site of disruption of the talin polypeptide, the other recognizing an epitope at the NH_2-terminal side of the disruption (Fig. 1 *A*). The two

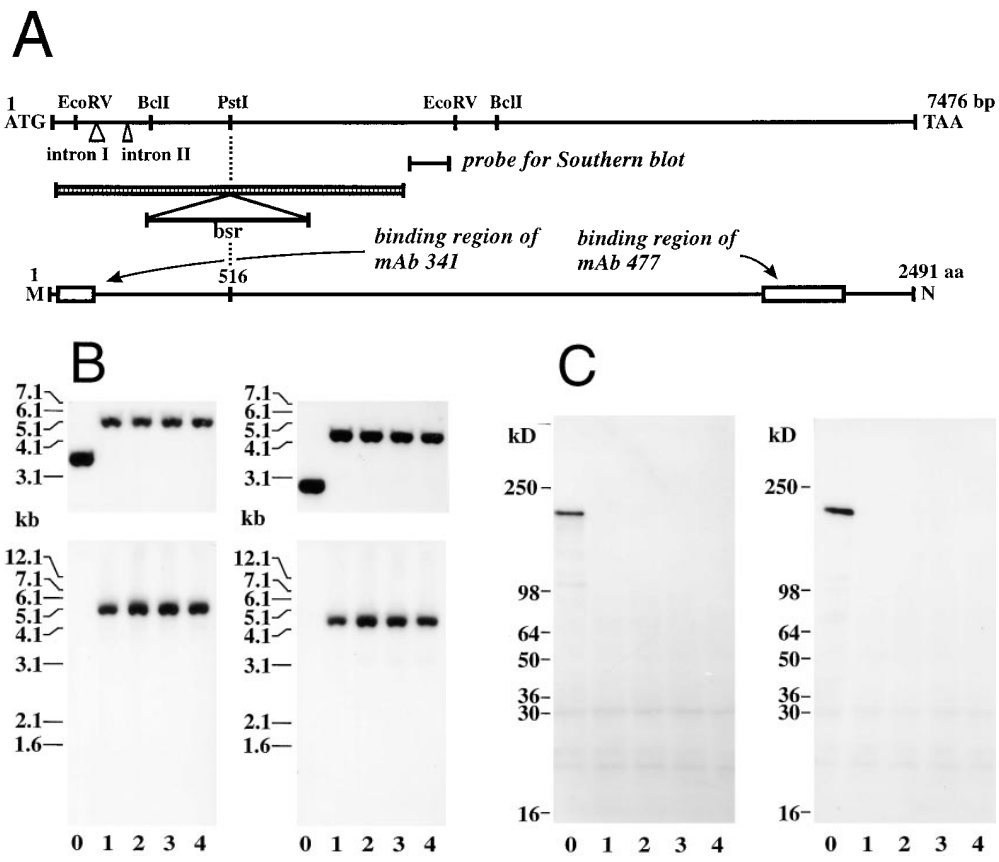

Figure 1. Generation of talin-null mutants by gene replacement. (*A*) Map of the talin gene of *D. discoideum*, the construct used for the talin knockout (*hatched*), the probe used to identify knockout mutants by Southern blotting, and location of two mAb binding sites at the protein. To produce the vector construct used for transfection, the blasticidin resistance (*bsr*) cassette was inserted into the PstI site of a genomic fragment comprising nucleotides 58–2,999 of the coding region. The PstI site resides in the codon for T516 of the talin sequence. The antibody binding regions were mapped by the use of bacterially expressed fragments. (*B*) Southern blots probed either with a fragment of the talin gene that flanks the 3′-end of the vector as indicated in *A* (*upper panels*), or with the bsr coding region (*lower panels*). Genomic DNA was digested with EcoRV (*left panels*) or BclI (*right panels*), according to the map in *A*. Lane numbers indicate wild-type AX2 (*0*), and four independent transformants HG1663–1666 (*1–4*). (*C*) Western blots of total cellular proteins of the same strains as in *B*. Proteins were separated by SDS-PAGE and probed with anti-talin mAb 477 (*left panel*) or mAb 341 (*right panel*). Talin in the wild-type runs at an apparent molecular mass of ~220 kD, although its calculated mass is 269 kD. Neither intact talin nor any fragment is detectable in the mutants. Since the promoter and the coding region up to amino acid 515 should not be affected by homologous recombination of the vector into the talin gene, the lack of an NH_2-terminal fragment appears to be due to instability of the transcript, inefficient translation, or degradation of the incomplete polypeptide.

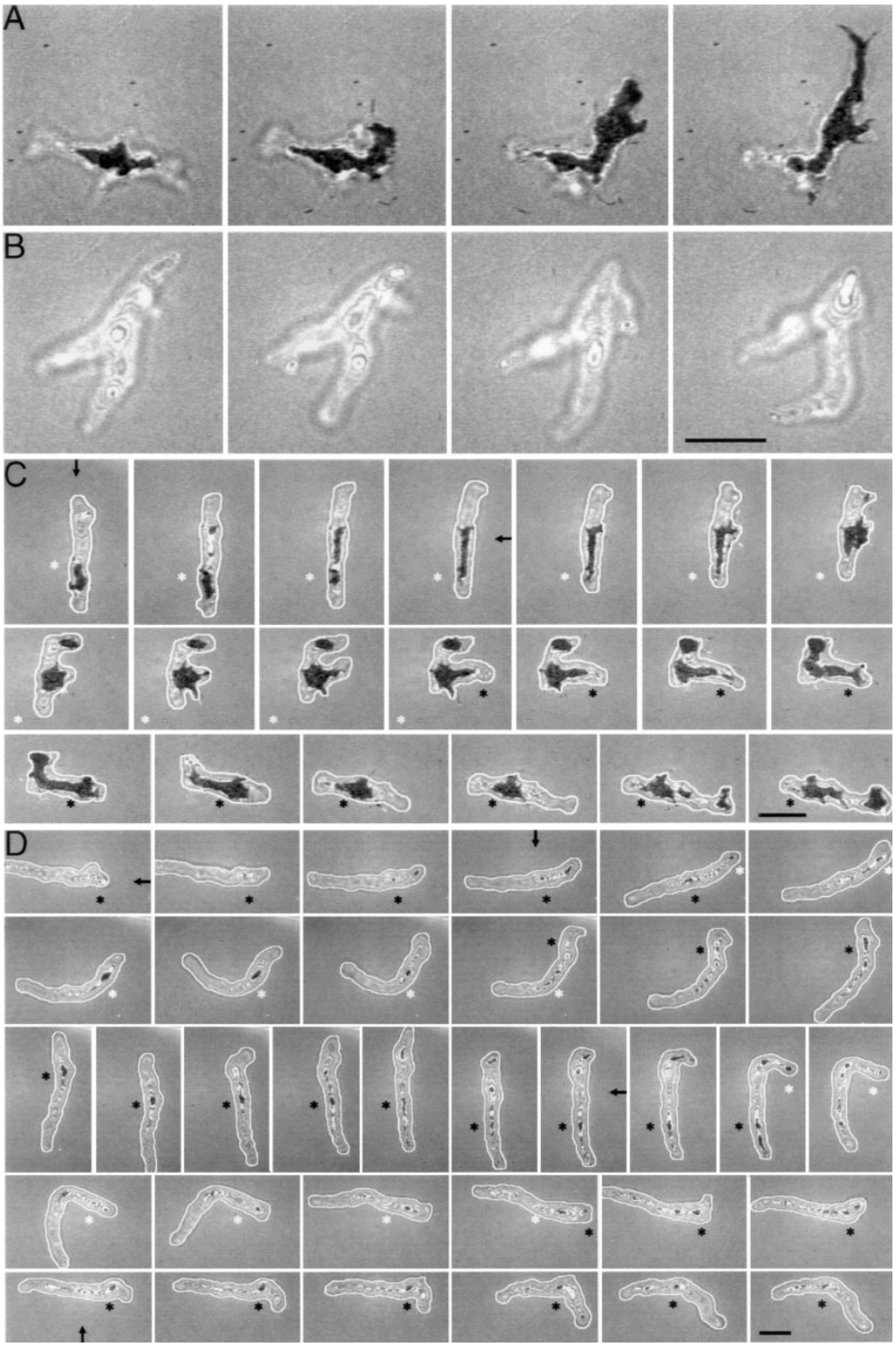

Figure 2. Cell-to-substrate adhesion, as visualized by RICM, and chemotactic responses in wild-type (*A* and *C*) and talin-null cells (*B* and *D*). Cells were starved for 6–8 h to induce development up to the aggregation-competent stage, and then allowed to settle on a BSA-coated glass surface. (*A* and *B*) Differences in cell-to-substrate adhesion exemplified by one wild-type and one talin-null cell, both freely moving on the glass surface in a fluid layer. The RICM images show black areas at sites of close contact of the wild-type cell with the substrate surface. Such areas are not seen in the RICM images of the talin-null cell, demonstrating the lack of close contact. The long lateral distances between the maxima of the interference patterns in the mutant cell indicate that major portions of the bottom surface of this cell formed small angles with the substrate surface. The rapid changes of these patterns reflect the instability of interactions with the substrate. (*C* and *D*) A wild-type and a talin-null cell exposed to changing gradients of chemoattractant. These cells were stimulated with cAMP through a micropipette, the tip of which was moved into different positions relative to the cells. Actual directions of the gradients are indicated by arrows. Despite its weak adhesion to the substrate, the talin-null cell was not slower than the wild-type cell: during straight movement toward the attractant, the front of the wild-type cell propagated with an average speed of 13 μm/min, and that of the talin-null cell with 17 μm/min. To make allowance for movement of the cells out of frame, white and black asterisks were introduced as stationary markers to denote points on the substrate. The cells were imaged using a double-view microscope (Weber et al., 1995). Contours of cell body projections were copied from bright-field images as white outlines into the RICM images. Intervals between the frames: 10 s. Bars, 10 μm.

antibodies no longer detected the talin band in the eight independent mutants, nor did the latter antibody recognize in the mutants any NH_2-terminal fragment of this protein that might originate from a truncated message (Fig. 1 *C*).

Impairment of Cell-to-Substrate Adhesion and the Chemotactic Response of Talin-Null Cells

A phenotypic alteration immediately obvious in the mutant cells was their weak adhesion to the polystyrol sur-

faces of plastic petri dishes, as revealed by their detachment upon gentle pipetting. To study this adhesion defect, alterations in the interaction of talin-null cells with a substrate surface were analyzed by RICM. Areas of close cell-to-substrate contact are visualized by RICM as dark areas (Gingell and Todd, 1979), which means that the reflecting cell surface approaches the glass surface with a distance <50 nm close to the zero order intensity minimum of the interference pattern (Rädler and Sackmann, 1993). The first interference maximum corresponding to a distance of λ/4 appears then as a bright area.

Glass coated with BSA proved to be of optimal adhesiveness for the motility of *D. discoideum* cells. This substrate allows wild-type cells to attach and detach in a regular pattern (Weber et al., 1995) and to move persistently with negligible loss of material retained on the substrate surface (Schindl et al., 1995). In the aggregation-competent stage, which is reached after several hours of starvation, wild-type cells adhere to the substrate only at portions of their basal surface, and the areas of contact rapidly change in size and shape with movement of the cells (Weber et al., 1995). An example is given in Fig. 2 *A*.

Talin-null cells had almost completely lost adhesiveness to BSA-coated glass. This is seen in RICM images by the absence of dark areas of contact in the center of interference patterns (Fig. 2 *B*). The finding that the area of closest approximation between the cell and substrate surfaces was regularly bright means that the distance was in the order of the first maximum of λ/4 = 136 nm for the green light used. This distance made firm attachment of the talin-null cells impossible, so that they easily drifted with slight convections in the fluid.

Aggregation-competent wild-type cells are highly responsive to cAMP as a chemoattractant, and cell-to-substrate interactions are highly dynamic during reorientation. The cells turn into a new direction by bending their established front or by extending a new front into the direction of the gradient. At the beginning of a chemotactic response, the front does not need to be in contact with the substrate, and sometimes two fronts compete with each other for becoming the leading edge (Weber et al., 1995). In the example shown in Fig. 2 *C*, the wild-type cell initially moved toward the top of the frames, then turned with its front toward the right, and shortly later produced a second front, which subsequently established itself as the leading edge. New sites of attachment at the fronts increased in size and fused with each other, followed by detachment at the tail of the cell.

Talin-null cells efficiently responded to cAMP by turning toward the source. Stimulation with the chemoattractant also slightly enhanced interaction with the substrate, so that grayish foci of attachment were seen in RICM images. However, the mutant cells were impaired in spreading and fusion of the contact areas (Fig. 2 *D*). Foci of attachment increased only marginally in size; often they were fixed in a position essentially stationary on the substrate, with the cells gliding ahead of these local sites of loose attachment. Most of the foci of cell-to-substrate contact in talin-null cells vanished when they had passed the middle of a cell. Some of the patches existed for up to 2 min, whereas others were short-lived and never reached the middle region of the cell.

A Conditional Defect in Phagocytosis Due to Reduced Cell-to-Particle Adhesion

Consequences of the adhesion defect in talin-null cells for particle uptake were assayed using heat-killed, fluorescently labeled yeast particles in shaken suspension. At a shaking frequency of 150 rpm, the rate of phagocytosis in talin-null cells was ~10% the rate in wild-type AX2 cells (Fig. 3 *A*). Assuming that this reduction in the rate of particle uptake is a consequence of impaired adhesion, one would predict a higher rate of uptake at conditions of low shear. Fig. 3 *B* shows that reducing the frequency of shaking from 150 to 100 rpm increased substantially the rate of particle uptake in talin-null cells and only moderately increased it in wild-type cells.

A particle adhering to a *Dictyostelium* cell triggers an extension of the cell surface that spreads as a cup-shaped lamella over the particle and finally engulfs it (Maniak et al., 1995). Uptake of liquid medium occurs in *D. discoideum* by macropinocytosis which, like phagocytosis, requires a response in the actin system to internalize a vesicle (Hacker et al., 1997). Macropinocytosis differs, however, from phagocytosis in being independent of the stimulus of a particle that impinges on the cell surface. To distinguish between a defect in adhesion and the process of uptake, internalization of TRITC-dextran, a fluid-phase marker, was measured. The rate of fluid-phase uptake proved to be indistinguishable in talin-null cells from that in wild-type cells (Fig. 3 *C*). Microscopic observations revealed that the mechanism of this uptake in talin-null cells is similar as recently described for wild-type cells (Hacker et al., 1997). Protrusions extending ⩾2 μm from the cell body eventually closed at their rim, thus entrapping an aliquot of medium (Fig. 3 *D*).

Surface Properties of Bacteria Critical for their Adhesion to Talin-Null Cells

Bacteria that differ in the carbohydrate moieties of their surface lipopolysaccharides are convenient probes to evaluate the role of adhesion in phagocytosis. When fixed in a lawn on an agar plate, a large variety of *E. coli* or *Salmonella* strains can support growth of *Dictyostelium* cells, independently of the chemical nature or physical properties of the bacterial surfaces. If applied in shaken suspension, adhesion of the bacteria to the phagocyte surface becomes crucial for uptake, since a bacterium needs to adhere until the phagocyte has produced a cup to envelop and eventually to engulf the bacterium. As far as wild-type cells of *D. discoideum* are concerned, the uptake of bacteria in suspension is primarily determined by surface lipopolysaccharides. Long polysaccharide chains prevent uptake by the lack of adhesion. It suffices to coat these carbohydrate chains with antibodies to render the bacteria appropriate for uptake in suspension (Gerisch et al., 1967).

E. coli B/r is commonly used for the efficient growth of *D. discoideum* wild-type cells in shaken suspension. The carbohydrate chains on the surface of this *E. coli* strain are reduced to a glucose-containing core oligosaccharide (Malchow et al., 1967). On a lawn of *E. coli B/r* on an agar plate, talin-null cells grew as fast as wild-type cells, which confirmed that engulfment of the bacteria is not impaired in the mutant cells (Fig. 4 *A*). In a suspension, however,

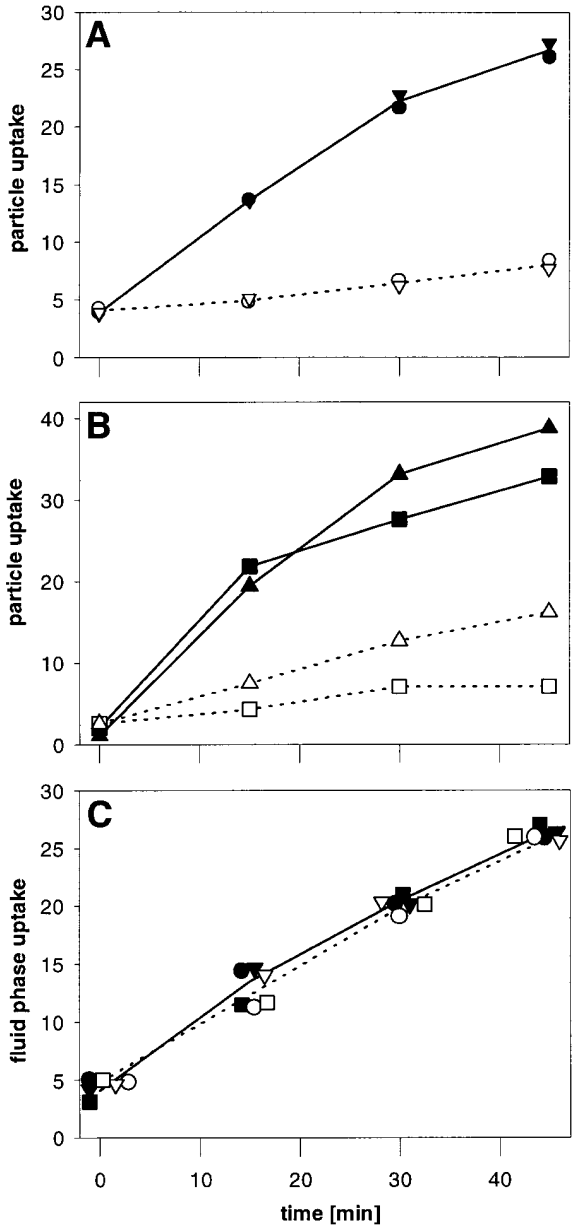

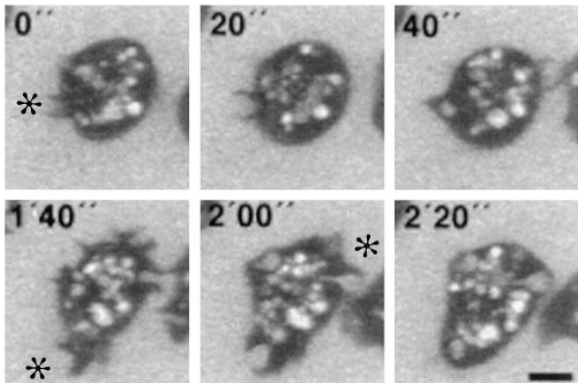

Figure 3. Reduced uptake rate of yeast particles contrasts to the normal rate of fluid-phase uptake in talin-null cells. Wild-type cells (*closed symbols*) and talin-null cells (*open symbols*) were incubated under shaking with heat-killed, TRITC-labeled yeast particles for phagocytosis, or with TRITC-labeled dextran for pinocytosis. (*A*) Time course of particle uptake by wild-type (●,▼) and talin-null cells (○, ▽), determined in two parallel experiments. Cells were shaken at 150 rpm with an excess of at least six yeast particles per wild-type or mutant cell. (*B*) Dependence of particle uptake on shearing stress. Wild-type (■, ▲) and talin-null (□, △) cells were incubated with yeast particles and shaken either at 150 rpm (■, □), as in *A*, or at 100 rpm (▲, △). (*C*) Time course of fluid-phase uptake determined in three parallel experiments (●, ▼, ■ and ○, ▽, □). (*D*) A talin-null cell taking up liquid medium by macropinocytosis. To visualize uptake, TRITC-dextran was added to the medium, and the cell was scanned by confocal fluorescence microscopy at the times indicated. The nonfluorescent cytoplasm is seen in black, the fluorescent medium in light grey, and endocytic vacuoles at grey-to-white values depending on the degree of concentration of the internalized TRITC-dextran. During the time period shown, the cell formed three macropinosomes in the confocal plane (*asterisks*). Bar, 5 μm.

the growth of talin-null cells on *E. coli B/r* was dramatically slowed down (Fig. 4 *B*).

To provide evidence that the core oligosaccharide present on the surface of *E. coli B/r* interfered with adhesion to talin-null cells, we used *Salmonella minnesota R595*, a strain appropriate for *D. discoideum* suspension cultures (Malchow et al., 1967; Gerisch et al., 1985; Cohen et al., 1994), which lacks the entire carbohydrate moiety apart from two residues of 3-deoxy-D-manno-octulosonic acid linked to lipid A (Lüderitz et al., 1966). In suspensions of this bacterial strain, the generation times of wild-type and talin-null mutant cells differed only slightly, indicating that bacteria of proper adhesiveness can be taken up by the mutant cells even under the restrictive conditions of a shaken suspension (Fig. 4 *C*).

The EDTA-sensitive Type of Cell-to-Cell Adhesion Is Talin Dependent

In suspension, undeveloped wild-type cells of *D. discoideum* aggregate into loose clusters. The cohesion of these cells is distinguished from that of aggregating cells by its EDTA sensitivity (Beug et al., 1973). Cell cohesion can be quantitatively assayed by an automated light scattering assay. Suspended cells are rotated in an agglutinometer in cuvettes that are designed to apply standardized shear to dissociate the cells (Beug and Gerisch, 1972). The strength of cell cohesion is then reflected in the size of aggregates formed against the dissociating forces, and the decrease of particle number accompanying aggregation results in reduced light scattering.

Fig. 5 *A* shows the behavior of undeveloped cells: when an equilibrium was reached after <1 h, light scattering in suspensions of wild-type cells was low in the absence and high in the presence of EDTA, whereas in suspensions of talin-null cells it was high both in the presence and absence of EDTA. The photographs of Fig. 5 *B* illustrate these quantitative data, indicating that the EDTA-sensitive cohesion of undeveloped cells is talin dependent.

In the aggregation-competent stage, talin-null cells adhered to each other in an EDTA-stable manner (Fig. 5 *C*), and the aggregates formed in suspension were only slightly smaller than those formed by wild-type cells (Fig. 5 *D*).

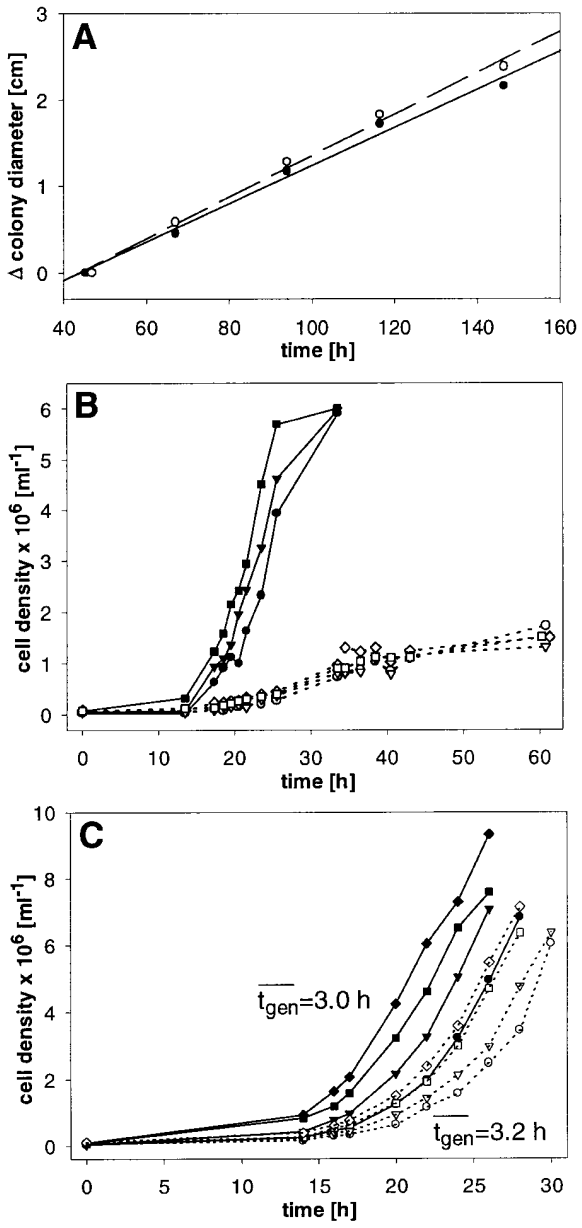

Figure 4. Growth of wild-type (*closed symbols*) and talin-null cells (*open symbols*) on bacteria. Two bacterial strains with different defects in lipopolysaccharide synthesis were used: *Salmonella minnesota R595* synthesizes only 2-keto-3-deoxyoctonate (3-deoxy-D-manno-octulosonic acid; KDO) linked to lipid A. *E. coli B/r* adds a core oligosaccharide consisting of heptose and glucose residues to this basal structure (Malchow et al., 1967). (*A*) Growth with *E. coli B/r* on agar plates. On lawns of bacteria, colony diameters increase linearly with time. Since the bacteria are completely used up by both wild-type and mutant cells at the border of the colonies, this increase is an indirect measure of uptake rates. Under these conditions, the growth rates of wild-type (●) and talin-null (○) cells were indistinguishable. Data are averages of 20 colonies measured for each strain. (*B*) Growth on *E. coli B/r* in suspension. Wild-type cells grew with a generation time of 3.4 h and entered the stationary phase upon consumption of the bacteria. Growth of talin-null cells became negligible after uptake of ~10% of the bacteria, as indicated by generation times >20 h. ◆ ◇, ■ □, ▼ ▽, and ● ○, cultures with inoculates of 9, 7, 5, and 3 × 10^4 cells per ml, respectively. (*C*) Growth on *Salmonella minnesota R595* in suspension under the same conditions as in *B*. On this bacterial strain, talin-null cells grew efficiently with only marginally longer generation times (t_{gen}) than wild-type cells. Symbols represent cultures inoculated with 8, 6, 4, and 2 × 10^4 cells per ml, in the same order as in *B*.

Cytokinesis Is Conditionally Impaired in Talin-Null Cells

The initial observation that talin-null cells become larger than wild-type cells when cultivated in suspension suggested a deficiency in cytokinesis. To establish this by quantitative data, numbers of nuclei were counted in cells that were cultivated either in suspension or on a glass surface. In suspension cultures, the majority of talin-null cells contained two to four nuclei, whereas wild-type cells were primarily mononucleated (Fig. 6, *top*). Under the same conditions, the average volume of talin-null cells was 1.5-fold that of wild-type cells. These results indicate that, in talin-null cells undergoing mitosis in suspension, cytokinesis fails to be reliably coupled to nuclear division. This deficiency was less distinct when cells grew on a solid surface (Fig. 6, *middle*), and it was not at all evident when the liquid medium was replaced as a source of nutrients by a lawn of bacteria on an agar surface (Fig. 6, *bottom*).

The finding that only a few of the talin-null cells acquired more than four nuclei in suspension culture with nutrient medium suggests a process that counterbalances the increase in nuclear number caused by the slight impairment of cytokinesis. To characterize this process, cytokinesis was recorded in bi- or multinucleated talin-null cells. Fig. 7 *A* illustrates mitosis in a binucleated cell that divided symmetrically into four daughter cells. In fixed preparations, mitotic stages of binucleated cells were characterized by the presence of two spindles and four asters of microtubules, which held variable positions relative to each other in the three-dimensional space of the cell body. In the three cells shown in Fig. 7 *B*, the two mitotic complexes, each consisting of a pair of asters connected to a spindle, were arranged in the same plane. These images illustrate most clearly that only two of the four cleavage furrows that are indistinguishable in Fig. 7 *A* are directed toward the middle of the spindles, the other pair incising the cell body in between the mitotic complexes.

In addition to binucleated cells, cells that contained three or four nuclei were found to form multiple spindles. It appears therefore that the increase in nuclear number is limited in talin-null cells by mitotic division cycles that give rise to more than two daughter cells. This type of cleavage is based on the shaping of cleavage furrows around the asters of microtubules.

Discussion

Differences in the Talin Dependency of Cell-to-Cell Adhesion Systems

Dictyostelium has been the first developmental system in which two types of cell-to-cell adhesion, an EDTA-stable and a sensitive one, could be distinguished (Gerisch, 1961) and shown to be blocked separately by antibody Fab (Beug et al., 1973). According to the data presented here,

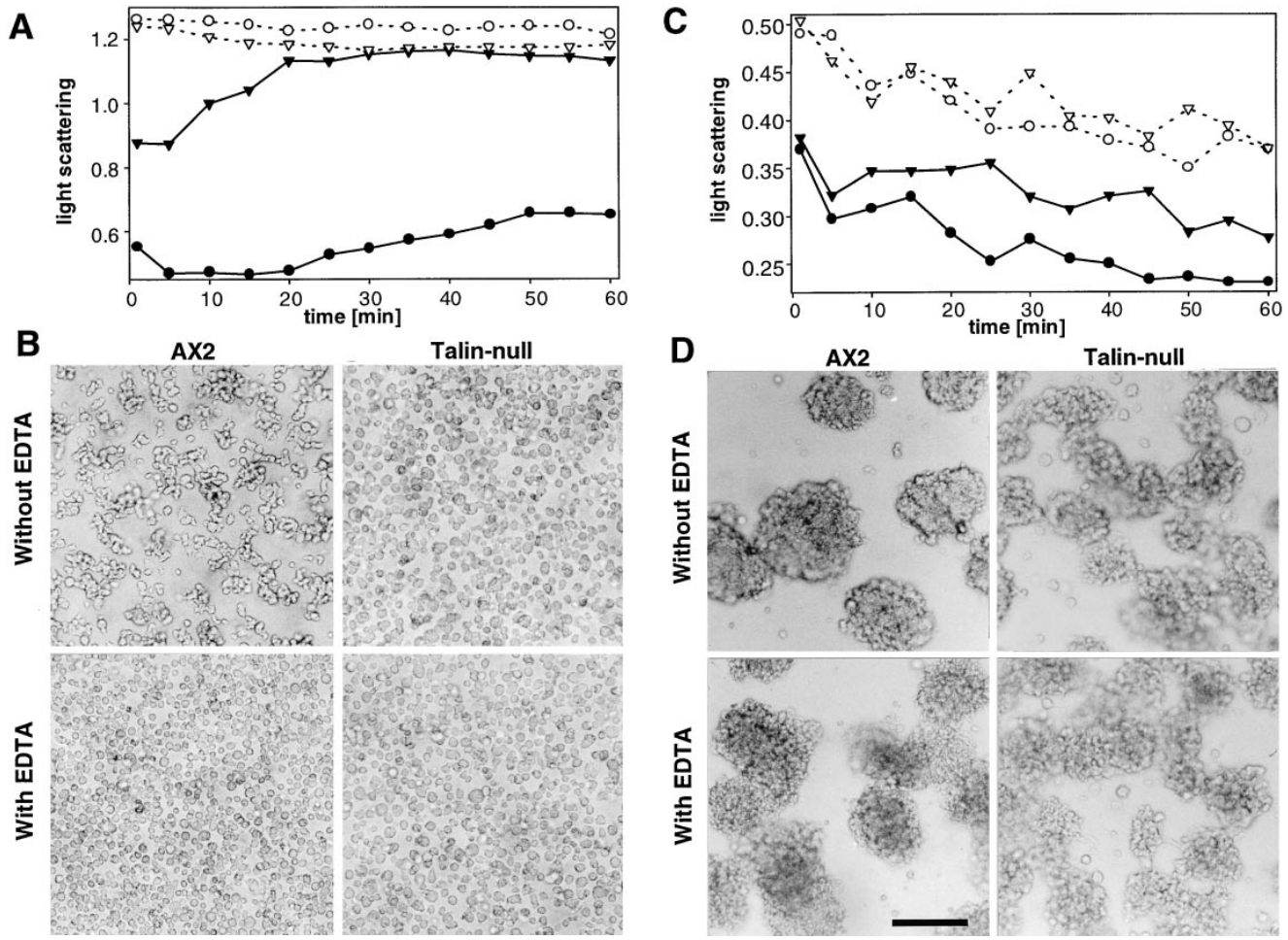

Figure 5. Cell-to-cell adhesion of undeveloped and aggregation-competent wild-type AX2 and talin-null cells in the absence and presence of EDTA. (*A*) Cell adhesion of undeveloped wild-type and talin-null cells, assayed in an agglutinometer to expose the cells to standardized shear forces. Within 1 h in the agglutinometer, equilibria of aggregated and single cells were obtained, as determined by light scattering measurements (Beug and Gerisch, 1972). Light scattering in arbitrary units indicates agglutination (low values) or dissociation into single cells (high values). Comparison of wild-type cells in the absence (●) and presence of 10 mM EDTA (▼) shows that cohesion of the undeveloped cells was sensitive to EDTA, in accordance with previous reports (Beug et al., 1973). Talin-null cells reached almost identical, high equilibrium values without (○) or with (▽) EDTA, indicating strong reduction of cohesiveness in these mutant cells. (*B*) Photographs of cell suspensions taken after 1 h of agitation in the agglutinometer. In wild-type AX2, irregularly shaped clusters of cells are recognizable in the absence of EDTA, and almost complete dissociation into single cells is seen with 10 mM EDTA (*left panels*). Nearly all of the talin-null cells remained single in the absence as in the presence of EDTA (*right panels*). (*C*) Cell adhesion of aggregation-competent wild-type (*closed symbols*) and talin-null cells (*open symbols*) in the absence (●, ○) or presence (▼, ▽) of 10 mM EDTA. (*D*) Illustration of EDTA-stable cell adhesion in wild-type AX2 and talin-null cells in the same experiment as shown in *C*. The developmentally regulated contact site A cell adhesion protein was expressed in the wild-type and mutant cells to the same level within a tolerance of 7% (data not shown). Bar (*B* and *D*), 100 μm.

the EDTA-sensitive "type B contacts" and also cell-to-substrate contacts represent talin-dependent types of cell adhesion (Fig. 5, *A* and *B*). Quantitative measurements confirmed that the energy of cell-to-substrate adhesion is strongly reduced in the talin-null cells of *Dictyostelium* (Simson, R., personal communication). A glycoprotein anchored to the membrane by a ceramide-based lipid (Stadler et al., 1989) is the major adhesion protein involved in the EDTA-stable cohesion of aggregating cells (Müller and Gerisch, 1978). Cell-to-cell adhesion mediated by this "contact site A" glycoprotein turned out to be rather independent of talin (Fig. 5, *C* and *D*).

In vertebrate cells talin interacts with integrins, which link the cell surface to receptors on the extracellular matrix (Beckerle and Yeh, 1990). The distinction of two adhesion systems in *Dictyostelium* on the basis of their linkage to talin suggests that also in this microorganism talin interacts as part of a specific complex with one type of adhesion protein in the plasma membrane. Integrins have not been identified in *Dictyostelium*; a candidate for a talin-regulated adhesion protein is a 126-kD (Chadwick et al., 1984) or 130-kD glycoprotein (Chia, 1996).

Whether or not *Dictyostelium* has a "protointegrin" on its surface is not only of phylogenetic interest but is also relevant for functional reasons. *Dictyostelium* cells manage in their natural habitat to move on soil particles of

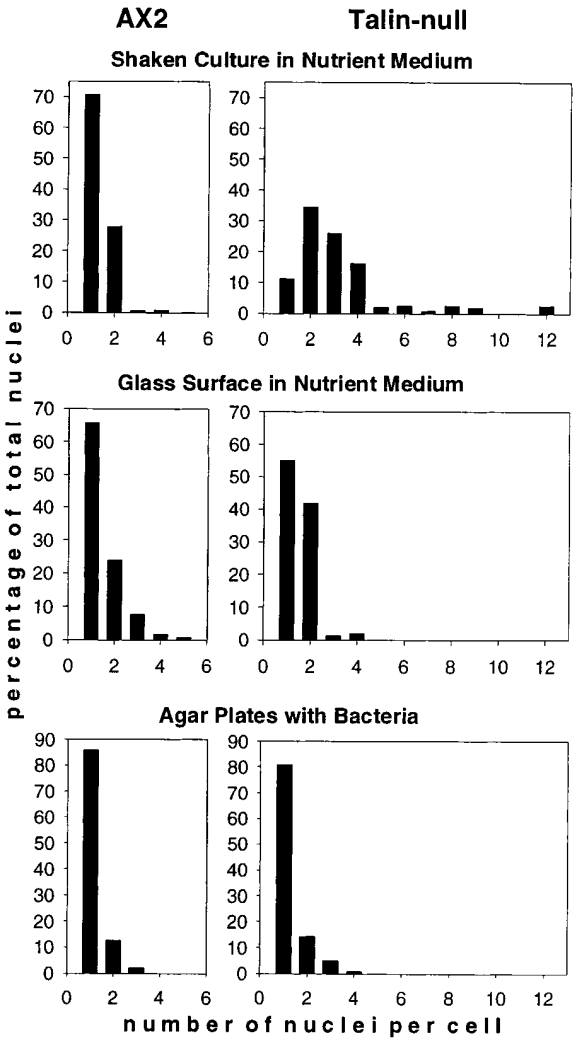

Figure 6. Histograms showing the probability of nuclei residing in mononucleated or multinucleated cells under various growth conditions. In wild-type AX2 (*left panels*), the majority of nuclei was located in mononucleated cells under all conditions tested. In talin-null strains (*right panels*) cultivated in shaken suspension culture, most of the nuclei were found in multinucleated cells carrying up to 12 nuclei. This tendency of talin-null cells to become multinucleated was less pronounced during growth in nutrient medium on a solid surface, and was undetectable during growth on agar plates in a lawn of *Klebsiella aerogenes.* For each panel, between 400 and 500 nuclei were counted in DAPI-stained cells.

varying chemical nature and physical surface properties. The question is whether *Dictyostelium* cells have a chance in their natural environment to use specific molecular interactions in regulating their adhesiveness to soil particles or to a variety of bacterial surfaces. There are several possibilities of how coupling of talin to a membrane protein regulates cell adhesion. (*a*) Adhesion might be regulated by clustering of the membrane protein, as it is known for integrins in other cells. (*b*) Some selectivity might be involved in the interaction of the putative adhesion protein with the surface of soil particles, analogous to the stereospecificity that determines attachment of *Xenopus* kidney cells to the surfaces of (R, R) and (S, S) enantiomorphous tartrate crystals (Hanein et al., 1994). (*c*) Thermally induced out-of-plane fluctuations of soft membranes lead to a repulsive force, which has the same distance dependence as the Van der Waals attractive forces (Sackmann, 1994). Coupling of the cell membrane to the actin cortex via talin will suppress the undulations, thereby increasing cell-to-substrate adhesion (Zeman et al., 1990). (*d*) Single cells of *Dictyostelium* might coat a surface with a secreted protein and then adhere on this layer in an analogous fashion to an integrin–fibronectin type of cell interaction with an extracellular matrix. In fact, a matrix is produced in the multicellular slug stage of *Dictyostelium* and is used as a surface for migration (Freeze and Loomis, 1977; Abe et al., 1994).

Cell Motility with a Minimum of Substrate Contact

The motility of fibroblasts or keratocytes depends on traction forces that these cells exert on their substrate (Oliver et al., 1994; Lauffenburger and Horwitz, 1996). The traction is thought to convert intracellularly generated contractile forces into net movement. Stress fibers and focal contacts appear to be optimized for efficient and directed pulling on the surrounding extracellular matrix. In contrast, aggregating cells of *D. discoideum* efficiently move while adhering only with part of their basal surface to the substrate. These cells lack static structures like stress fibers or focal adhesion complexes and are fast moving with speeds of up to 30 μm/min. In talin-null cells, substrate adhesion is even further reduced to an absolute minimum (Fig. 2). These almost nonadhesive cells exemplify a case of cell motility largely uncoupled from traction forces.

For the movement of talin-null cells on small patches of contact with a substrate, the following possibilities can be considered. First, loose adhesion might induce a local response, e.g., coupling of a membrane patch immobilized on the substrate to one of the myosins, so that this patch is driven in the membrane in a rearward direction (Jay and Elson, 1992). As a result, the cell will move ahead while the patch remains stationary on the substrate. Second, cell locomotion might be effected by a continuous membrane flux, either in the form of a rolling movement (Anderson et al., 1996) or a lipid flow generated by exocytosis at the front and by endocytosis along the lateral cell surface (Bretscher, 1996). Talin-null cells offer themselves for a detailed analysis of membrane events essential for cell locomotion because of the absence of spreading, which in wild-type cells masks the local interactions at small areas of cell-to-substrate contact.

Mutants to Dissect Phagocytosis

Phagocytosis mutants may be classified into four major groups: (*a*) those deficient in the adhesion of particles to the phagocyte surface, (*b*) mutants altered in signal transduction from the cell surface to the cortical cytoskeleton, (*c*) cytoskeletal mutants impaired in the mechanism of particle uptake, and (*d*) mutants in proteins that play a role in later steps of the phagocytic pathway. To begin with the third category, a series of gene disruption mutants has been generated in *Dictyostelium* to eliminate proteins associated with the actin system. These proteins include coronin, which accumulates together with actin early at

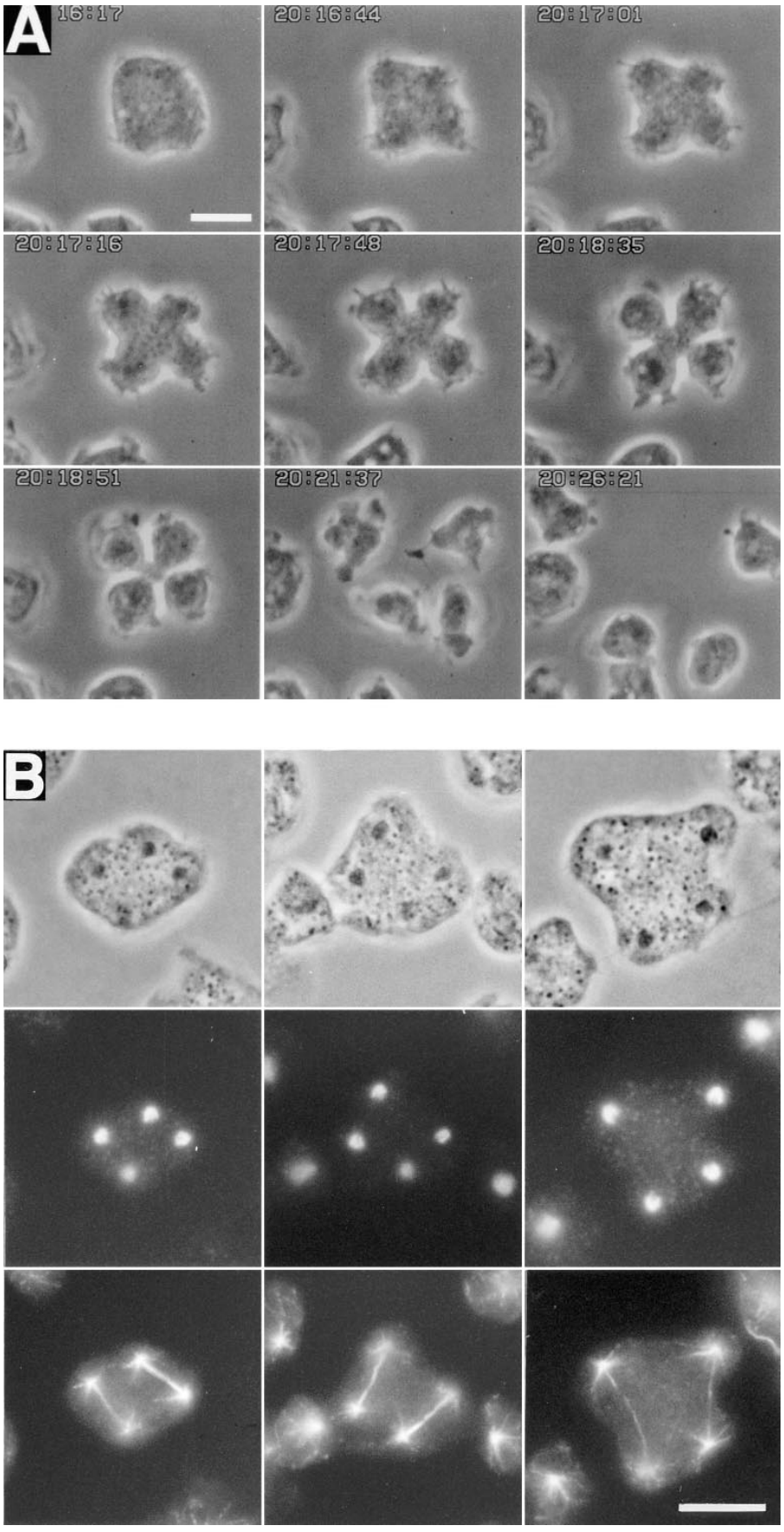

Figure 7. Mitotic division of binucleated talin-null cells. (*A*) Sequence of shape changes of one cell dividing into four. Numbers on the video record show that for progression of the cleavage furrow from the second to the seventh frame ~2 min was required. (*B*) Anaphase and telophase stages of three binucleated cells shown in phase contrast (*top*), stained with DAPI for DNA (*middle*), and labeled with anti–α-tubulin antibody to depict spindles and microtubule asters (*bottom*). Bar, 10 μm.

the phagocytic cup (Maniak et al., 1995) and later reassociates with postlysosomal endosomes (Rauchenberger et al., 1997), and two F-actin cross-linking proteins, 120-kD gelation factor (ABP120) and α-actinin (Cox et al., 1996; Rivero et al., 1996). Since integrity of the actin system is essential for phagocytosis to occur (Maniak et al., 1995), the lack of proteins that cross-link actin filaments or otherwise contribute to the viscoelastic properties of the actin cortex most likely affects particle uptake directly.

On the basis of the following results, we propose that the talin-null cells are impaired in the initial adhesion to a particle and in subsequent spreading on its surface. The rate at which yeast particles are taken up by talin-null cells in shaken suspension can be markedly increased by reducing the frequency of shaking (Fig. 3 *B*). This inverse dependence of uptake on the strength of shear indicates that the average persistence time of a particle at the phagocyte surface is shorter than the time a cell would need to irreversibly entrap the particle. Extreme differences in the uptake rate of bacteria that differ in their surface properties provide a second argument for an impairment of adhesiveness in talin-null cells (Fig. 4). Fluid-phase uptake shows that talin-null cells can form surface extensions and convert them into macropinosomes large enough to include a bacterium (Fig. 3 *D*). In suspensions of 10^{10} bacteria per ml, as used in our experiments, accidental uptake will supply the cells with not more than one bacterium per 100 macropinosomes filled only with buffer. This explains why talin-null cells are almost unable to grow on *E. coli B/r* in suspension, whereas they are perfectly capable of growing in a dense lawn of the same bacteria on an agar surface. By the same argument, it is the strong adhesiveness of the carbohydrate-deficient *R595* strain of *Salmonella minnesota* that allows the talin-null cells to recruit these bacteria efficiently from a suspension.

Wild-type cells of *D. discoideum* extend a lamella with a speed of ~10 μm/min around a particle. This process is controlled by a zipper mechanism; it can be interrupted at any stage before closure of a phagocytic vesicle (Maniak et al., 1995). If the assumption is correct that the initial stages of phagocytosis resemble the spreading of a motile cell on a planar substrate (Grinnell, 1984), one can deduce from the dotlike contacts that talin-null cells form on a substrate that phagocytosis is similarly altered by weak initial adhesion and insufficient spreading of the mutant cells on a particle surface. Along the same line, it has been inferred from the enrichment of talin in phagocytic cups of mouse macrophages that talin plays a role during F_c receptor–mediated phagocytosis in linking transmembrane receptors to the force-generating cytoskeleton (Greenberg et al., 1990), similar to its implication in focal adhesion assembly.

In several of the previously isolated phagocytosis mutants of *Dictyostelium*, the protein affected is unknown, and inactivation of talin appears to be one possibility. Mutants characterized by Cohen et al. (1994) do not grow in suspensions of *S. minnesota R595*, which distinguishes the defect in these mutants from the impaired adhesion of talin-null cells. Mutants selected earlier by Vogel et al. (1980) differ from the talin-null mutants by their ability to grow in suspensions of *E. coli B/r*. Two separate adhesion mechanisms are involved in the binding of these bacteria to *Dictyostelium* cells, one unspecific and a sugar-specific one. If the unspecific type of adhesion is eliminated by mutagenesis of *D. discoideum* cells, bacteria of the *E. coli B/r* type can still stick to the mutant cells by virtue of terminal glucose residues on their lipopolysaccharides (Vogel et al., 1980). These and other sugar residues are recognized by lectinlike receptors exposed on *Dictyostelium* cell surfaces (Bozzaro and Roseman, 1983). The fact that talin-null cells are almost incapable of growing on *E. coli B/r* in suspension implies that talin is linked to both adhesion systems, the sugar-specific and the unspecific one.

Cytokinesis in Talin-Null Cells

As in other eukaryotic cells, cytokinesis in *D. discoideum* involves the formation of a cleavage furrow that initiates separation of the daughter cells. Our data indicate that talin, as an actin-associated protein, supports formation of the cleavage furrow. Impairment of cytokinesis in talin-null cells that grow in shaken suspension indicates a role for talin in cytoskeletal functions distinct from its involvement in making the cells adhesive. In the suspension cultures, a high proportion of bi- to tetranucleated cells is observed (Fig. 6).

Changes in cell shape during cytokinesis are brought about by the actin-rich cell cortex in conjunction with the microtubule-based spindle and asters. The synchronous division of multiple nuclei in a talin-null cell clearly reveals that a cleavage furrow is induced wherever two asters of microtubules are placed adjacent to each other (Fig. 7). This finding extends observations made on a *Dictyostelium* mutant lacking myosin II (Neujahr et al., 1997). Mitosis in multinucleated cells of this mutant is accompanied by folding of the cell surface around each aster of microtubules.

The cleavage stages in talin-null cells resemble experimentally disordered stages in dividing eggs of the sand dollar, *Arbacia lixula* (Rappaport, 1986). If in these eggs the formation of a cleavage furrow is prevented during the first nuclear division by dislocating the mitotic apparatus, four furrows are simultaneously induced during the second division at spaces between the asters, giving rise to four blastomers. In *Arbacia* blastomers as well as *Dictyostelium* cells, cruciform stages are diagnostic of single cells dividing into four. The spindle is dispensable in these cases for a cleavage furrow to be formed, and it is the apposition of two asters closely associated with the cell cortex that induces a furrow at the midline between them. Since this effect is easily observed in talin-null cells, these cells may provide a tool to identify the proteins or molecular configurations that specify a cleavage furrow.

We thank Alicija Baskaya for mAb production, Gerhard Rahn for iodination, and Jean-Marc Schwartz for digitalization of the video images.

Received for publication 14 April 1997 and in revised form 16 May 1997.

References

Abe, T., A. Early, F. Siegert, C. Weijer, and J. Williams. 1994. Patterns of cell movement within the *Dictyostelium* slug revealed by cell type-specific, surface labeling of living cells. *Cell.* 77:687–699.

Albigès-Rizo, C., P. Frachet, and M.R. Block. 1995. Down regulation of talin alters cell adhesion and the processing of the α5β1 integrin. *J. Cell Sci.* 108: 3317–3329.

Anderson, K.I., Y.L. Wang, and J.V. Small. 1996. Coordination of protrusion

and translocation of the keratocyte involves rolling of the cell body. *J. Cell Biol.* 134:1209–1218.
Beckerle, M.C., and R.K. Yeh. 1990. Talin: role at sites of cell-substratum adhesion. *Cell Motil. Cytoskeleton.* 16:7–13.
Bertholdt, G., J. Stadler, S. Bozzaro, B. Fichtner, and G. Gerisch. 1985. Carbohydrate and other epitopes of the contact site A glycoprotein of *Dictyostelium discoideum* as characterized by monoclonal antibodies. *Cell Differ.* 16: 187–202.
Beug, H., and G. Gerisch. 1972. A micromethod for routine measurement of cell agglutination and dissociation. *J. Immunol. Methods.* 2:49–57.
Beug, H., F.E. Katz, and G. Gerisch. 1973. Dynamics of antigenic membrane sites relating to cell aggregation in *Dictyostelium discoideum. J. Cell Biol.* 56: 647–658.
Bozzaro, S., and S. Roseman. 1983. Adhesion of *Dictyostelium discoideum* cells to carbohydrates immobilized in polyacrylamide gels. *J. Biol. Chem.* 258: 13882–13889.
Bozzaro, S., R. Merkl, and G. Gerisch. 1987. Cell adhesion: its quantification, assay of the molecules involved, and selection of defective mutants in *Dictyostelium* and *Polysphondylium. Methods Cell Biol.* 28:359–385.
Bretscher, M.S. 1996. Getting membrane flow and the cytoskeleton to cooperate in moving cells. *Cell.* 87:601–606.
Burridge, K., and L. Connell. 1983. A new protein of adhesion plaques and ruffling membranes. *J. Cell Biol.* 97:359–367.
Burridge, K., and P. Mangeat. 1984. An interaction between vinculin and talin. *Nature (Lond.).* 308:744–746.
Chadwick, C.M., J.E. Ellison, and D.R. Garrod. 1984. Dual role for *Dictyostelium* contact site B in phagocytosis and developmental size regulation. *Nature (Lond.).* 307:646–647.
Chia, C.P. 1996. A 130-kDa plasma membrane glycoprotein involved in *Dictyostelium* phagocytosis. *Exp. Cell Res.* 227:182–189.
Claviez, M., K. Pagh, H. Maruta, W. Baltes, P. Fisher, and G. Gerisch. 1982. Electron microscopic mapping of monoclonal antibodies on the tail region of *Dictyostelium* myosin. *EMBO (Eur. Mol. Biol. Organ.) J.* 1:1017–1022.
Cohen, C.J., R. Bacon, M. Clarke, K. Joiner, and I. Mellman. 1994. *Dictyostelium discoideum* mutants with conditional defects in phagocytosis. *J. Cell Biol.* 126:955–966.
Cox, D., D. Wessels, D.R. Soll, J. Hartwig, and J. Condeelis. 1996. Re-expression of ABP-120 rescues cytoskeletal, motility, and phagocytosis defects of ABP-120(−) *Dictyostelium* mutants. *Mol. Biol. Cell.* 7:803–823.
DePasquale, J.A., and C.S. Izzard. 1991. Accumulation of talin in nodes at the edge of the lamellipodium and separate incorporation into adhesion plaques at focal contacts in fibroblasts. *J. Cell Biol.* 113:1351–1359.
Freeze, H., and W.F. Loomis. 1977. The role of the fibrillar component of the surface sheath in the morphogenesis of *Dictyostelium discoideum. Dev. Biol.* 56:184–194.
Geiger, B., S. Yehuda-Levenberg, and A.D. Bershadsky. 1995. Molecular interactions in the submembrane plaque of cell-cell and cell-matrix adhesions. *Acta Anat.* 154:46–62.
Gerisch, G. 1961. Zellfunktionen und Zellfunktionswechsel in der Entwicklung von *Dictyostelium discoideum.* V. Stadienspezifische Zellkontaktbildung und ihre quantitative Erfassung. *Exp. Cell Res.* 25:535–554.
Gerisch, G., and H.U. Keller. 1981. Chemotactic reorientation of granulocytes stimulated with micropipettes containing fMet-Leu-Phe. *J. Cell Sci.* 52:1–10.
Gerisch, G., O. Lüderitz, and E. Ruschmann. 1967. Antikörper fördern die Phagozytose von Bakterien durch Amöben. *Zsch. Naturforschung.* 22b:109.
Gerisch, G., U. Weinhart, G. Bertholdt, M. Claviez, and J. Stadler. 1985. Incomplete contact site A glycoprotein in HL220, A modB mutant of *Dictyostelium discoideum. J. Cell Sci.* 73:49–68.
Gingell, D., and I. Todd. 1979. Interference reflection microscopy. A quantitative theory for image interpretation and its application to cell substratum measurement. *Biophys. J.* 26:507–526.
Goldmann, W.H., A. Bremer, M. Häner, U. Aebi, and G. Isenberg. 1994. Native talin is a dumbbell-shaped homodimer when it interacts with actin. *J. Struct. Biol.* 112:3–10.
Greenberg, S., K. Burridge, and S.C. Silverstein. 1990. Colocalization of F-actin and talin during F_c receptor-mediated phagocytosis in mouse macrophages. *J. Exp. Med.* 172:1853–1856.
Grinnell, F. 1984. Fibroblast spreading and phagocytosis: similar cell responses to different-sized substrata. *J. Cell. Physiol.* 119:58–64.
Hacker, U., R. Albrecht, and M. Maniak. 1997. Fluid-phase uptake by macropinocytosis in *Dictyostelium. J. Cell Sci.* 110:105–112.
Hanein, D., B. Geiger, and L. Addadi. 1994. Differential adhesion of cells to enantiomorphous crystal surfaces. *Science (Wash. DC).* 263:1413–1416.
Hemmings, L., D.J.G. Rees, V. Ohanian, S.J. Bolton, A.P. Gilmore, B. Patel, H. Priddle, J.E. Trevithick, R.O. Hynes, and D.R. Critchley. 1996. Talin contains three actin-binding sites each of which is adjacent to a vinculin-binding site. *J. Cell Sci.* 109:2715–2726.
Hock, R.S., J.M. Sanger, and J.W. Sanger. 1989. Talin dynamics in living microinjected nonmuscle cells. *Cell Motil. Cytoskeleton.* 14:271–287.
Horwitz, A., K. Duggan, C. Buck, M.C. Beckerle, and K. Burridge. 1986. Interaction of plasma membrane fibronectin receptor with talin: a transmembrane linkage. *Nature (Lond.).* 320:531–533.
Humbel, B.M., and E. Biegelmann. 1992. A preparation protocol for postembedding immunoelectron microscopy of *Dictyostelium discoideum* cells with monoclonal antibodies. *Scanning Microsc.* 6:817–825.
Isenberg, G., V. Niggli, U. Pieper, S. Kaufmann, and W.H. Goldmann. 1996. Probing phosphatidylinositolphosphates and adenosinenucleotides on talin nucleated actin polymerization. *FEBS Lett.* 397:316–320.
Jay, P.Y., and E.L. Elson. 1992. Surface particle transport mechanism independent of myosin II in *Dictyostelium. Nature (Lond.).* 356:438–440.
Jockusch, B.M., P. Bubeck, K. Giehl, M. Kroemker, J. Moschner, M. Rothkegel, M. Rüdiger, K. Schlüter, G. Stanke, and J. Winkler. 1995. The molecular architecture of focal adhesions. *Annu. Rev. Cell Dev. Biol.* 11:379–416.
Kaufmann, S., T. Piekenbrock, W.H. Goldmann, M. Bärmann, and G. Isenberg. 1991. Talin binds to actin and promotes filament nucleation. *FEBS Lett.* 284: 187–191.
Kaufmann, S., J. Käs, W.H. Goldmann, E. Sackmann, and G. Isenberg. 1992. Talin anchors and nucleates actin filaments at lipid membranes. *FEBS Lett.* 314:203–205.
Kilmartin, J.V., B. Wright, and C. Milstein. 1982. Rat monoclonal antitubulin antibodies derived by using a new nonsecreting rat cell line. *J. Cell Biol.* 93: 576–582.
Knezevic, I., T.M. Leisner, and S.C.-T. Lam. 1996. Direct binding of the platelet integrin $\alpha_{IIb}\beta_3$ (GPIIb-IIIa) to talin. *J. Biol. Chem.* 271:16416–16421.
Kreitmeier, M., G. Gerisch, C. Heizer, and A. Müller-Taubenberger. 1995. A talin homologue of *Dictyostelium* rapidly assembles at the leading edge of cells in response to chemoattractant. *J. Cell Biol.* 129:179–188.
Kupfer, A., S.L. Swain, and S.J. Singer. 1987. The specific direct interaction of helper T cells and antigen-presenting B cells. II. Reorientation of the microtubule organizing center and reorganization of the membrane-associated cytoskeleton inside the bound helper T cells. *J. Exp. Med.* 165:1565–1580.
Lauffenburger, D.A., and A.F. Horwitz. 1996. Cell migration: a physically integrated molecular process. *Cell.* 84:359–369.
Lewis, J.M., and M.A. Schwartz. 1995. Mapping in vivo associations of cytoplasmic proteins with integrin β1 cytoplasmic domain mutants. *Mol. Biol. Cell.* 6: 151–160.
Lüderitz, O., C. Galanos, H.J. Risse, E. Ruschmann, S. Schlecht, G. Schmidt, H. Schulte-Holthausen, R. Wheat, O. Westphal, and J. Schlosshardt. 1966. Structural relationship of *Salmonella* O and R antigens. *Ann. NY Acad. Sci.* 133:349–374.
Malchow, D., O. Lüderitz, O. Westphal, G. Gerisch, and V. Riedel. 1967. Polysaccharide in vegetativen und aggregationsreifen Amöben von *Dictyostelium discoideum.* I. In vivo Degradierung von Bakterien-Lipopolysaccharid. *Eur. J. Biochem.* 2:469–479.
Maniak, M., R. Rauchenberger, R. Albrecht, J. Murphy, and G. Gerisch. 1995. Coronin involved in phagocytosis: dynamics of particle-induced relocalization visualized by a green fluorescent protein tag. *Cell.* 83:915–924.
Moulder, G.L., M.M. Huang, R.H. Waterston, and R.J. Barstead. 1996. Talin requires β-integrin, but not vinculin, for its assembly into focal adhesion-like structures in the nematode *Caenorhabditis elegans. Mol. Biol. Cell.* 7:1181–1193.
Muguruma, M., S. Matsumura, and T. Fukazawa. 1990. Direct interactions between talin and actin. *Biochem. Biophys. Res. Commun.* 171:1217–1223.
Müller, K., and G. Gerisch. 1978. A specific glycoprotein as the target site of adhesion blocking Fab in aggregating *Dictyostelium* cells. *Nature. (Lond.).* 274: 445–449.
Neujahr, R., C. Heizer, and G. Gerisch. 1997. Myosin II-independent processes in mitotic cells of *Dictyostelium discoideum*: redistribution of the nuclei, rearrangement of the actin system and formation of the cleavage furrow. *J. Cell Sci.* 110:123–137.
Niggli, V., S. Kaufmann, W.H. Goldmann, T. Weber, and G. Isenberg. 1994. Identification of functional domains in the cytoskeletal protein talin. *Eur. J. Biochem.* 224:951–957.
Noegel, A., D.L. Welker, B.A. Metz, and K.L. Williams. 1985. Presence of nuclear associated plasmids in the lower eukaryote *Dictyostelium discoideum. J. Mol. Biol.* 185:447–450.
Nuckolls, G.H., L.H. Romer, and K. Burridge. 1992. Microinjection of antibodies against talin inhibits the spreading and migration of fibroblasts. *J. Cell Sci.* 102:753–762.
Oliver, T., J. Lee, and K. Jacobson. 1994. Forces exerted by locomoting cells. *Semin. Cell Biol.* 5:139–147.
Rädler, J., and E. Sackmann. 1993. Imaging optical thicknesses and separation distances of phospholipid vesicles at solid surfaces. *J. Phys. II France.* 3:727–748.
Rappaport, R. 1986. Establishment of the mechanism of cytokinesis in animal cells. *Int. Rev. Cytol.* 105:245–281.
Rauchenberger, R., U. Hacker, J. Murphy, J. Niewöhner, and M. Maniak. 1997. Coronin and vacuolin identify consecutive stages of a late, actin-coated endocytic compartment in *Dictyostelium. Curr. Biol.* 7:215–218.
Rivero, F., B. Köppel, B. Peracino, S. Bozzaro, F. Siegert, C.J. Weijer, M. Schleicher, R. Albrecht, and A.A. Noegel. 1996. The role of the cortical cytoskeleton: F-actin crosslinking proteins protect against osmotic stress, ensure cell size, cell shape and motility, and contribute to phagocytosis and development. *J. Cell Sci.* 109:2679–2691.
Sackmann, E. 1994. Membrane bending energy concept of vesicle- and cell-shapes and shape-transitions. *FEBS Lett.* 346:3–16.
Schindl, M., E. Wallraff, B. Deubzer, W. Witke, G. Gerisch, and E. Sackmann. 1995. Cell-substrate interactions and locomotion of *Dictyostelium* wild-type and mutants defective in three cytoskeletal proteins: a study using quantitative reflection interference contrast microscopy. *Biophys. J.* 68:1177–1190.

Stadler, J., T.W. Keenan, G. Bauer, and G. Gerisch. 1989. The contact site A glycoprotein of *Dictyostelium discoideum* carries a phospholipid anchor of a novel type. *EMBO (Eur. Mol. Biol. Organ.) J.* 8:371–377.

Sutoh, K. 1993. A transformation vector for *Dictyostelium discoideum* with a new selectable marker, bsr. *Plasmid.* 30:150–154.

Sydor, A.M., A.L. Su, F.-S. Wang, A. Xu, and D.G. Jay. 1996. Talin and vinculin play distinct roles in filopodial motility in the neuronal growth cone. *J. Cell Biol.* 134:1197–1207.

Takeuchi, K., A. Kawashima, A. Nagafuchi, and S. Tsugita. 1994. Structural diversity of band 4.1 superfamily members. *J. Cell Sci.* 107:1921–1928.

Vogel, G., L. Thilo, H. Schwarz, and R. Steinhart. 1980. Mechanism of phagocytosis in *Dictyostelium discoideum*: phagocytosis is mediated by different recognition sites as disclosed by mutants with altered phagocytic properties. *J. Cell Biol.* 86:456–465.

Weber, I., and R. Albrecht. 1997. Image processing for combined bright-field and reflection interference contrast video microscopy. *Comput. Programs Biomed.* 53:113–118.

Weber, I., E. Wallraff, R. Albrecht, and G. Gerisch. 1995. Motility and substratum adhesion of *Dictyostelium* wild-type and cytoskeletal mutant cells: a study by RICM/bright-field double-view image analysis. *J. Cell Sci.* 108: 1519–1530.

Winkler, J., H. Lünsdorf, and B.M. Jockusch. 1997. Energy-filtered electron microscopy reveals that talin is a highly flexible protein composed of a series of globular domains. *Eur. J. Biochem.* 243:430–436.

Zeman, K., H. Engelhard, and E. Sackmann. 1990. Bending undulations and elasticity of the erythrocyte membrane: effects of cell shape and membrane organization. *Eur. Biophys. J.* 18:203–219.

Zhang, J., R.M. Robson, J.M. Schmidt, and M.H. Stromer. 1996. Talin can crosslink filaments into both networks and bundles. *Biochem. Biophys. Res. Commun.* 218:530–537.